ISSN 0031-918X, Physics of Metals and Metallography, 2017, Vol. 118, No. 10, pp. 935–945. © Pleiades Publishing, Ltd., 2017.
Original Russian Text © A.G. Popov, D.A. Kolodkin, V.S. Gaviko, D.Yu. Vasilenko, A.V. Shitov, A.V. Vlasyuga, M.Yu. Govorkov, D.Yu. Bratushev, 2017, published in Fizika Metallov i Metallovedenie, 2017, Vol. 118, No. 10, pp. 981–992.

ELECTRICAL AND MAGNETIC PROPERTIES

High-Power (Nd, Dy)–(Fe, Co)–B Magnets with a Low Temperature Coefficient of Induction

A. G. Popov[a, b], D. A. Kolodkin[a, *], V. S. Gaviko[a, b], D. Yu. Vasilenko[c], A. V. Shitov[c], A. V. Vlasyuga[c], M. Yu. Govorkov[c], and D. Yu. Bratushev[c]

[a] *Institute of Metal Physics, Ural Branch, Russian Academy of Sciences, ul. S. Kovalevskoi 18, Ekaterinburg, 620990 Russia*
[b] *Yeltsin Ural Federal University, ul. Mira 19, Ekaterinburg, 620002 Russia*
[c] *Ural Electromechanical Plant, ul. Studencheskaya 9, Ekaterinburg, 620137 Russia*
**e-mail: kolodkin@imp.uran.ru*

Received January 24, 2017; in final form, April 4, 2017

Abstract—High-power (Nd, Dy)–(Fe, Co)–B permanent magnets with a low temperature coefficient of induction (α) were prepared using advantages of strip casting and low-oxygen technologies. The microstructure and temperature dependences of magnetic properties have been studied on sintered $(Nd_{1-x}Dy_x)_{13.9}(Fe_{1-y}Co_y)_{79.8}Cu_{0.1}Ga_{0.1}B_{6.1}$ magnets with $0.20 \le x \le 0.25$ and $0 \le y \le 0.20$. The increase in y from 0 to 0.20 is accompanied by an increase in the Curie temperature from 327 to 492°C. This favors a decrease in the value of α from 0.099 to 0.060%/°C, respectively. Magnets with an oxygen content of no more than 2500 ppm which were prepared from the $(Nd_{0.75}Dy_{0.25})_{13.9}(Fe_{0.85}Co_{0.15})_{79.8}Cu_{0.1}\,Ga_{0.1}B_{6.1}$ alloy, have the following hysteresis characteristics at 140°C: $B_r \ge 11.3$ kG, $H_c \ge 8$ kOe, and $(BH)_{max} \ge 30$ MGOe; in this case, $\alpha \le |-0.07\%/°C|$.

Keywords: permanent magnet, coercive force, magnetic susceptibility, Curie temperature

DOI: 10.1134/S0031918X1710009X

INTRODUCTION

High-power Nd–Fe–B permanent magnets are widely used in different technical devices. However, due to the low Curie temperature of the main magnetic $Nd_2Fe_{14}B$ phase ($T_C = 310$°C), these magnets are characterized by low temperature stability of hysteresis properties. The values of temperature coefficients of induction (TCI) (α) and coercivity (β) are –0.12 and –0.60%/°C for a temperature range of 20–100°C, respectively [1]. This disadvantage substantially limits the scope of applications of Nd–Fe–B magnets at high temperatures. Ways to improve the temperature stability of Nd–Fe–B magnets are well known and available in [2–6]. The partial substitution of cobalt for iron favors an increase of T_C and a decrease in the modulus of value α, while the partial substitution of dysprosium for neodymium allows one to increase the anisotropy field H_A and coercive force H_c [5, 6]. In particular, magnets characterized by rather low TCI magnitudes of α = –0.028 and –0.020%/°C were prepared from the $(Nd_{0.6}Dy_{0.4})_{16}(Fe_{0.7}Co_{0.3})_{78}B_6$ [7] and $(Nd_{0.52}Dy_{0.48})_{15}(Fe_{0.66}Co_{0.34})_{76}Al_1B_6$ [8] alloys, respectively. However, magnetic characteristics at both room temperature and an operating temperature of ~150°C were found to be lower than those for Sm–Co–Fe–Cu–Zr magnets. At the same time, magnets for some applications, in particular for high-torque electrical motors, are required to possess a combination of high maximum energy product ($(BH)_{max} > 30$ MGOe), adequate TCI (α ~ –0.07%/°C), and high mechanical strength. Only Nd–Fe–B magnets can ensure this combination of characteristics. The aim of the present study is to prepare high-power (Nd, Dy)–(Fe, Co)–B permanent magnets with a decreased TCI using advantages of strip casting [9–11] and low-oxygen [12] technologies.

EXPERIMENTAL

Alloys $(Nd_{0.75}Dy_{0.25})_{13.9}(Fe_{1-x}Co_x)_{79.8}Cu_{0.1}Ga_{0.1}B_{6.1}$ (at %) containing 0–14.2 wt % Co and $(Nd_{0.73}Dy_{0.27})_{14.5}(Fe_{0.85}Co_{0.15})_{79}Cu_{0.1}Ga_{0.3}B_{6.1}$ were prepared in the form of flakes ~0.3 mm thick using strip casting technique. After hydrogen decrepitation, the alloys were subjected to jet milling in nitrogen to obtain a powder with the average particle size D_p = 3.05–3.15 μm. Powders placed in a matrix were compacted in a magnetic field of 15 kOe applied perpendicular to the compacting force. The use of special equipment for the low-oxygen preparation technology allowed us to ensure a low oxygen content in the powder, which is no more than 1000 ppm at all stages of the preparation process and interoperational processing. Green compacts were sintered in a vacuum at a temperature of 1065–1075°C and additionally

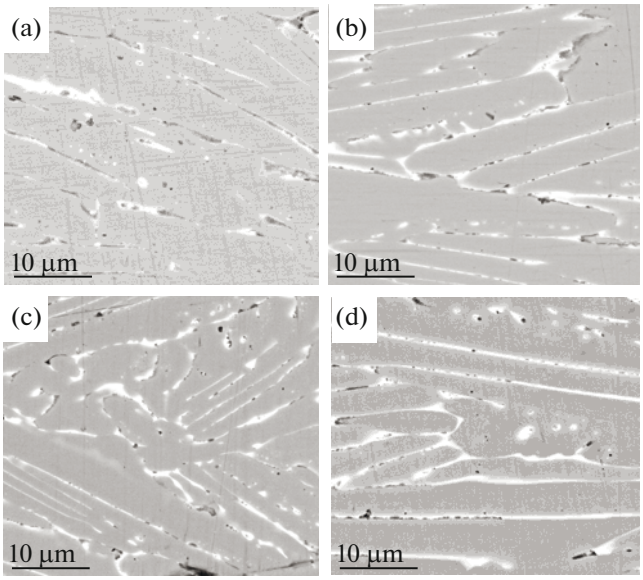

Fig. 1. Microstructure of platelike $(Nd_{0.75}Dy_{0.25})_{13.9}(Fe_{1-x}Co_x)_{79.8}Cu_{0.1}Ga_{0.1}B_{6.1}$ alloys (strip casting) with x equal to (a) 0, (b) 0.10, (c) 0.15, and (d) 0.20.

annealed at 880°C for 1 h and subsequently at 510°C for 2 h. Magnetization reversal curves were measured in a closed magnetic circuit of a Permagraph L installation in a temperature range of 22–180°C. The Curie temperature of the starting alloys and sintered magnets was determined using temperature dependences of magnetic susceptibility, which were measured in an ac magnetic field of 10 Oe with a frequency of 800 Hz using a transformer method and measuring compensation coils. The microstructure and the element-concentration distribution in alloy flakes and sintered magnets were studied using TSCAN VEGA 2LMH and QUANTA-200 scanning electron microscopes equipped with microprobe analyzers. X-ray diffraction data were obtained using a DRON-6M diffractometer and Cr $K\alpha$ radiation.

RESULTS AND DISCUSSION

Microstructure of Strip-Casting Alloys

Figure 1 shows the microstructure of the $(Nd_{0.75}Dy_{0.25})_{13.9}(Fe_{1-x}Co_x)_{79.8}Cu_{0.1}Ga_{0.1}B_{6.1}$ alloy flake in the center of the section perpendicular to the flake plane. The right sides of micrographs correspond to the contact surface of flakes (the surface in contact with a quenching wheel during casting). A fan-shaped dendritic structure of the main-phase grains (gray in color) is observed. Table 1 shows the chemical composition of the phase, which was determined ignoring the boron content. The ratio of the total content of rare-earth metals (R = Nd + Dy) to that of other elements (M) is 1 : 7 and, therefore, the composition of the phase corresponds to the $(Nd, Dy)_2(Fe, Co)_{14}B$ (2 : 14 : 1) stoichiometry. Bright lamellae enriched in rare-earth elements and depleted of iron run through the grains of the main phase. As the cobalt content in the alloys increases, the cobalt concentration in both main and lamellar phases increases (Fig. 2). In this case, cobalt is mainly located in the lamellar phase, and the cobalt content in it is 2–5% higher than that in the 2 : 14 : 1 phase. The Dy concentration in the lamellar phase slightly increases, whereas the total content of rare-earth elements decreases, and the R : M ratio becomes close to the 1 : 2 stoichiometry. This agrees with the appearance of additional X-ray diffraction reflections that correspond to the Laves phase with the $MgCu_2$-type structure in the X-ray diffraction pattern for alloy with x = 0.2. As is known, the Laves phase is not formed in the Nd–Fe system, but it is stabilized in $(Nd,°Dy)(Fe, Co)_2$ compounds as the concentration of both Dy and Co increases [13].

Table 1. Data of electron microprobe analysis for $(Nd_{0.75}Dy_{0.25})_{13.9}(Fe_{1-x}Co_x)_{79.8}Cu_{0.1}Ga_{0.1}B_{6.1}$ alloys prepared by strip-casting technique

Co content		Phase	Chemical composition, wt %	Formula
x	wt %			
0	0	Gray (2 : 14 : 1)	22.1Nd 7.0Dy 70.3Fe 0.1Co 0.5Al	$RM_{6.5}$
		Bright	59.8Nd 2.9Dy 29.8Fe 1.6Co 5.1Ga 0.8Al	$RM_{1.5}$
0.10	7.1	Gray (2 : 14 : 1)	22.0Nd 7.1Dy 63.8Fe 6.6Co 0.5Al	$RM_{7.1}$
		Bright	54.3Nd 4.9Dy 30.9Fe 9.20Co 0.1Ga 0.6Al	$RM_{1.7}$
0.15	10.7	Gray (2 : 14 : 1)	22.8Nd 6.5Dy 59.8Fe 10.3Co 0.6Al	$RM_{6.4}$
		Bright	51.6Nd 4.7Dy 31.3Fe 11.8Co 0.2Ga 0.4Al	$RM_{2.0}$
0.20	14.2	Gray (2 : 14 : 1)	21.4Nd 6.7Dy 57.4Fe 14.0Co 0.5Al	$RM_{6.8}$
		Bright	46.3Nd 7.8Dy 25.8Fe 19.5Co 0.2Ga 0.40Al	$RM_{2.2}$

Magnetic Properties

Figure 3 shows temperature dependences of the magnetic susceptibility $\chi(T)$ and temperature derivative of magnetic susceptibility $d\chi/dT$ for starting alloys and sintered magnets. The Curie temperature T_C was determined as the temperature corresponding to the minimum in the $d\chi/dT$ curves in Fig. 3b. The starting alloys with $x = 0$ and prepared magnets have the same $T_C = 327$°C. As the cobalt content increases to $x = 0.2$, the Curie temperature increases almost linearly by more than 150°C (Fig. 3c); for sintered magnets, it is 10°C higher than that for the initial alloys.

Figure 4 shows the magnetization reversal curves for magnets with cobalt contents of $x = 0$–0.2, which were measured at temperatures of 23–180°C. These curves were used to determine the temperature dependences of residual induction B_r and magnetization coercivity H_{cJ}, which are given in Figs. 5a and 5b, respectively. Table 2 gives the temperature coefficients of residual induction (α) and coercive force (β) for different temperature ranges calculated by the expressions

$$\alpha = [(B_r(T) - B_r(23))/(B_r(23)(T - 23))] \times 100\%; \quad (1)$$

$$\beta = [(H_{cJ}(T) - H_{cJ}(23))/(H_{cJ}(23)(T - 23))] \times 100\%. \quad (2)$$

As the Curie temperature of sintered magnets increases, the descent rate dB_r/dT decreases (Fig. 5a). This leads to a monotonic decrease in the modulus of α. For example, for the practically important temperature range of 23–140°C, the modulus of TCI for alloys with the cobalt content of $x = 0$–0.20 decreases from 0.099 to 0.060%/°C, respectively. At the same time, the modulus of the temperature coefficient β increases for all temperature ranges. These variations of α and β agree with the dependences of B_r, H_{cJ}, and $(BH)_{max}$ on the cobalt content for sintered magnets, which were measured at 23 and 140°C. The B_r and $(BH)_{max}$ parameters measured at room temperature progressively decrease as the cobalt content increases; at 140°C, the parameters increase and, at $x = 0.15$, reach maximum magnitudes of 11.6 kG and 30.9 MGOe, respectively.

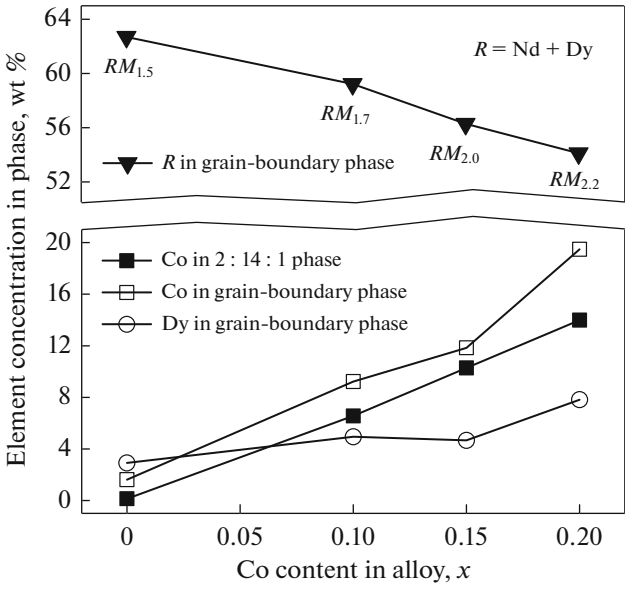

Fig. 2. Dependences of element concentrations of 2 : 14 : 1 and lamellar phases on the total Co content in the alloy.

The H_{cJ} (x) values monotonically decrease at both 23 and 140°C by 42 and 58%, respectively. As a result, the H_{cJ} values (in CGSM units) become lower than the B_r values. This fact indicates the appearance of a critical condition for the self-demagnetization of magnets in magnetic systems even with a low demagnetization coefficient $B/H \sim 2$, which limits the operating conditions of the magnets at high temperatures.

We perform a simple qualitative analysis of the reasons for the decrease in H_c with an increasing cobalt content using an expression that characterizes the magnetization reversal of (Nd, Dy)–(Fe, Co)–B magnets via the mechanism of nucleation as follows [5, 14]:

$$H_c(x) = aH_A(x) - 4\pi N_{eff}M_s(x), \quad (3)$$

where $H_A(x)$ is the anisotropy field, a is the structural parameter that characterizes the decrease in the nucle-

Table 2. Values of temperature coefficients α and β for $(Nd_{0.75}Dy_{0.25})_{13.9}(Fe_{1-x}Co_x)_{79.8}Cu_{0.1}Ga_{0.1}B_{6.1}$ magnets

Temperature range,°C	Co content in alloy, x							
	$x = 0$		$x = 0.10$		$x = 0.15$		$x = 0.20$	
	α, %/°C	β, %/°C	α, /°C	β, %/°C	α, /°C	β, %/°C	α, /°C	β, %/°C
23–60	–0.073	–0.527	–0.059	–0.596	–0.067	–0.691	–0.030	–0.718
23–90	–0.082	–0.510	–0.067	–0.611	–0.072	–0.646	–0.051	–0.648
23–120	–0.091	–0.478	–0.072	–0.578	–0.071	–0.580	–0.055	–0.604
23–140	–0.099	–0.473	–0.077	–0.553	–0.072	–0.549	–0.060	–0.573
23–160	–0.104	–0.460	–0.083	–0.526	–0.074	–0.519	–0.061	–0.539
23–180	–0.112	–0.448	–0.087	–0.499	–0.078	–0.489	–0.065	–0.509

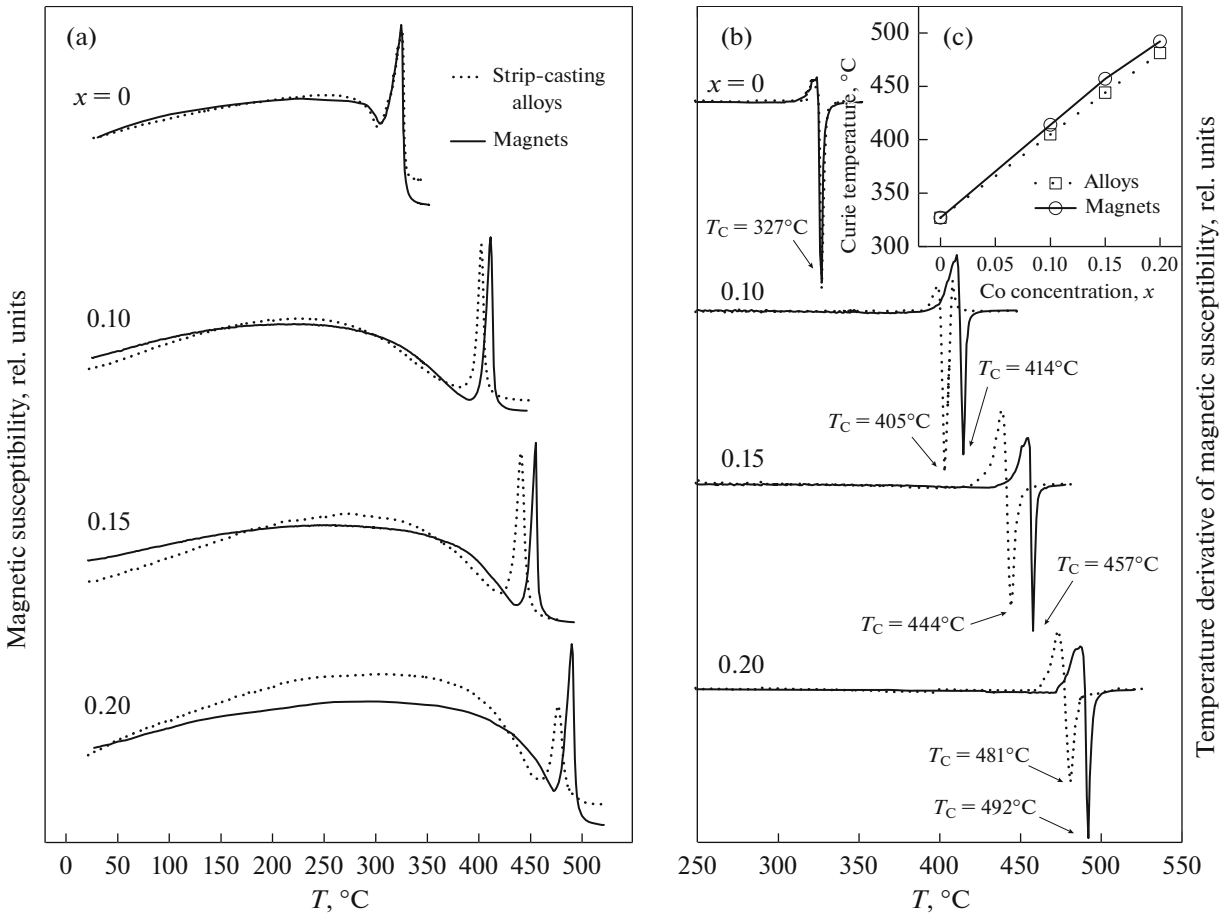

Fig. 3. Temperature dependences of (a) magnetic susceptibility and (b) temperature derivative of magnetic susceptibility for starting $(Nd_{0.75}Dy_{0.25})_{13.9}(Fe_{1-x}Co_x)_{79.8}Cu_{0.1}Ga_{0.1}B_{6.1}$ alloys (strip casting) and sintered magnets. (c) Inset shows the dependence of the Curie temperature on the Co concentration.

ation field due to the presence of crystallographic defects at the grain surface, and $M_s(x)$ is the saturation magnetization. The effective local demagnetizing factor N_{eff} is determined by the degree of texture, grain shape, and other parameters of microstructure. It follows from the literature data that the H_A magnitude for the $Nd_2(Fe_{1-x}Co_x)_{14}B$ compounds at room temperature only decreases by 5% as Co substitutes for Fe to $x = 0.20$ [3, 5]. The contribution of the second term in Eq. (3) to the decrease in the coercive force, which is related to the increase in the concentration $4\pi M_s(x)$ of the $Nd_2(Fe_{1-x}Co_x)_{14}B$ compounds can be only 6%. At the same time, as is shown in Fig. 6b, the coercivity of the studied $(Nd_{0.75}Dy_{0.25})_{13.9}(Fe_{1-x}Co_x)_{79.8}Cu_{0.1}Ga_{0.1}B_{6.1}$ magnets, which was measured at 23°C, decreases by 42% as x increases to 0.20. Thus, the magnitudes of structure-sensitive coefficients in Eq. (3) do not remain unchanged. Coefficient a should decrease, whereas the N_{eff} coefficient should increase with increasing x. This is likely to be predetermined by changes in the microstructure of magnets.

Phase Composition and Microstructure of Sintered Magnets

Figure 7 shows X-ray diffraction patterns for powder samples prepared from the $(Nd_{0.75}Dy_{0.25})_{13.9}(Fe_{1-x}Co_x)_{79.8}Cu_{0.1}Ga_{0.1}B_{6.1}$ magnets with $x = 0$, 0.15, and 0.20. Table 3 shows the results of phase analysis and lattice parameters of the phases. The lattice parameters a and c of the main tetragonal 2 : 14 : 1 phase decrease with increasing Co content; this agrees with the literature data in [2, 15]. At the same time, the volume fraction of the 2 : 14 : 1 phase decreases from 99 to 95 vol %. In addition to the reflections of the 2 : 14 : 1 phase, the X-ray diffraction patterns of all samples indicate additional reflections of the fcc phase (with the NaCl-type structure), which is usually related to the RO_x oxide.

The lattice parameter $a \approx 5.07$ Å of the phase is almost unchanged as the cobalt content increases. The volume fraction of the phase increases from 1 to 2.5 vol % for compounds with $x = 0$–0.20, respectively. The X-ray diffraction pattern of magnet with $x = 0.15$ exhibits weak reflections corresponding to the cubic Laves

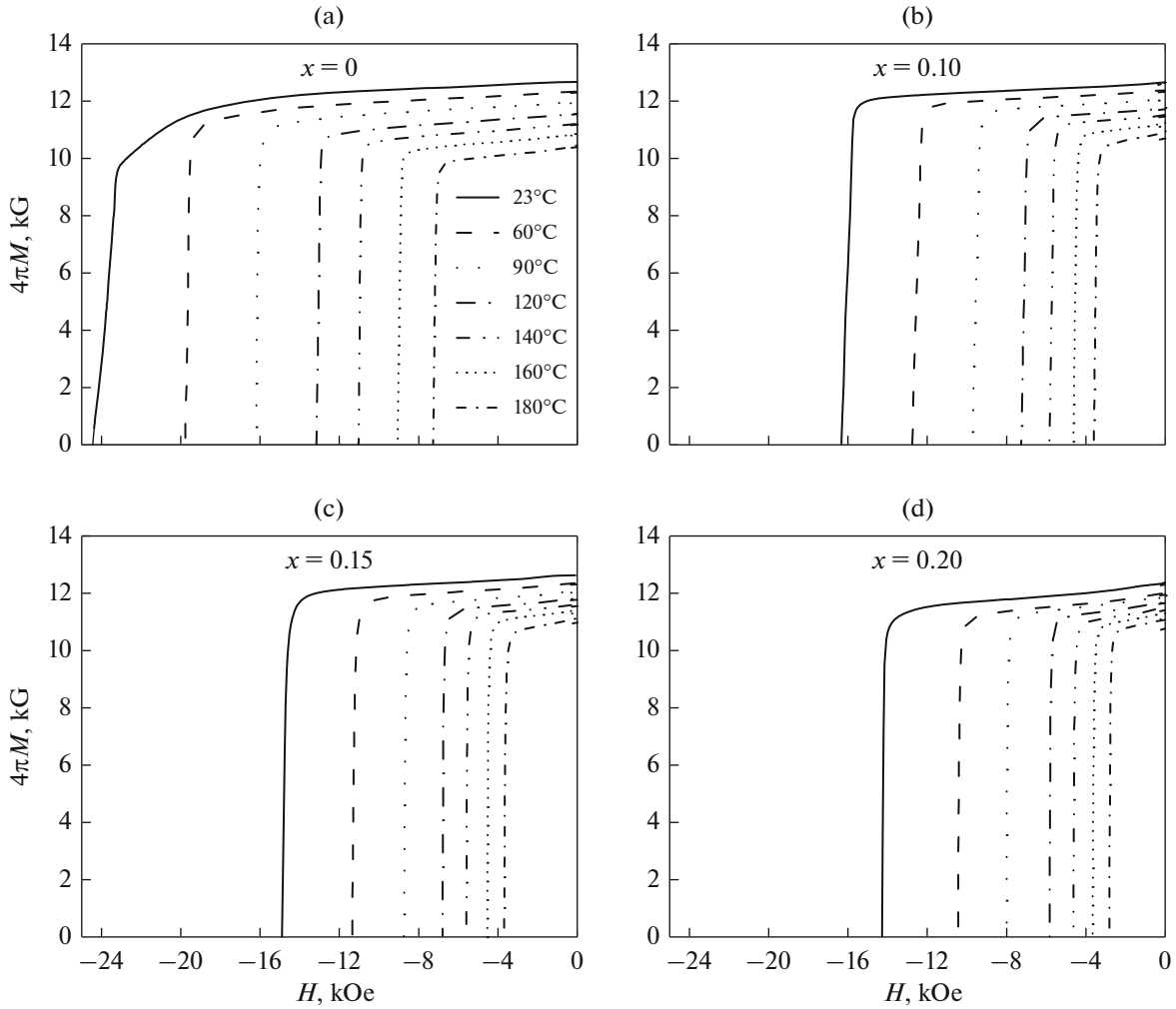

Fig. 4. Magnetization reversal curves measured in a temperature range of 23–180°C for sintered magnets prepared from the $(Nd_{0.75}Dy_{0.25})_{13.9}(Fe_{1-x}Co_x)_{79.8}Cu_{0.1}Ga_{0.1}B_{6.1}$ alloys with x equal to (a) 0, (b) 0.10, (c) 0.15, and (d) 0.20.

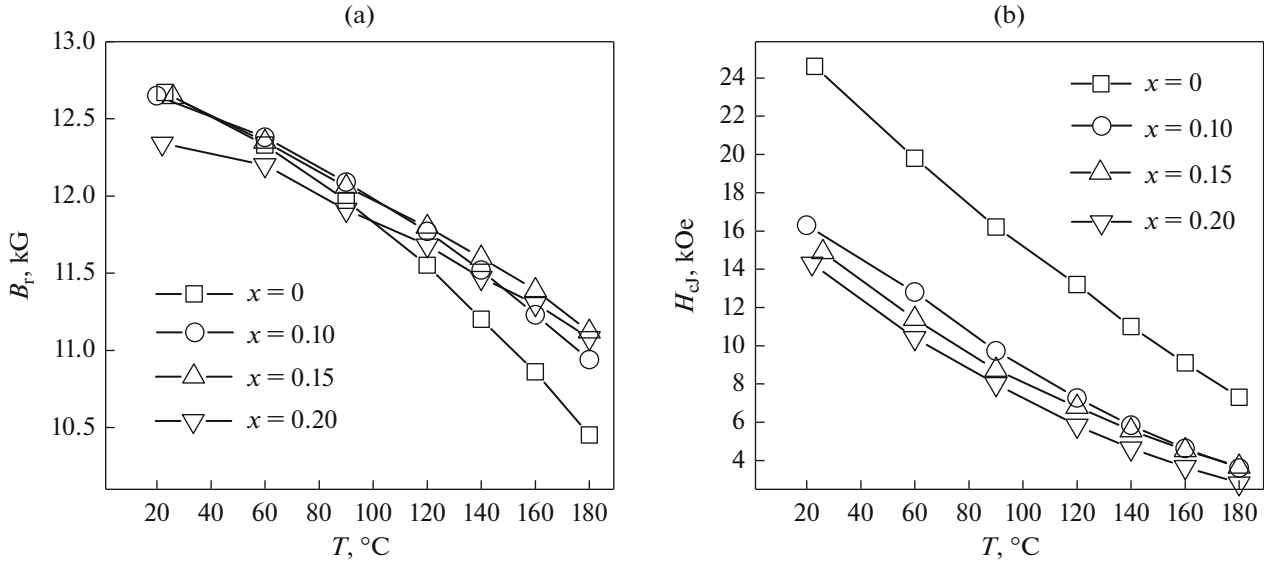

Fig. 5. Temperature dependences of (a) residual induction and (b) magnetization coercivity for sintered $(Nd_{0.75}Dy_{0.25})_{13.9}(Fe_{1-x}Co_x)_{79.8}Cu_{0.1}Ga_{0.1}B_{6.1}$ magnets.

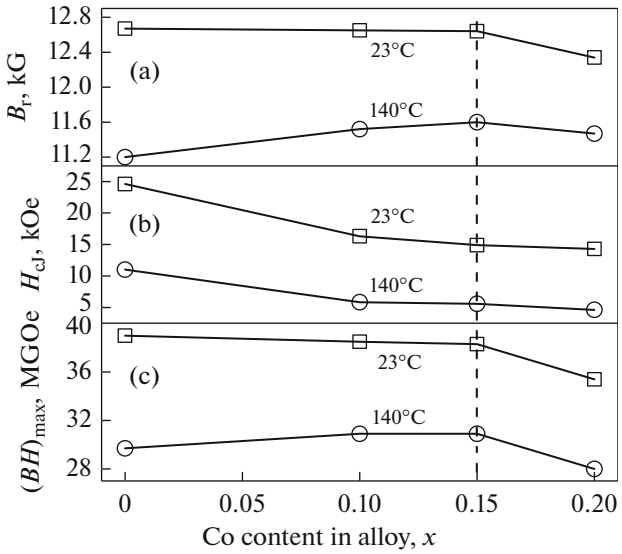

Fig. 6. Dependences of B_r, H_{cJ}, and $(BH)_{max}$ on the Co content in sintered magnets.

phase of the $MgCu_2$-type phase (RM_2). As x increases to 0.20, the RM_2-phase reflections shift to high-angle (2Θ) range; this fact indicates a decrease in the lattice parameter a and, therefore, the increase in the Co content in this phase.

Figure 8 shows the microstructure of sintered magnets prepared from the $(Nd_{0.75}Dy_{0.25})_{13.9}(Fe_{1-x}Co_x)_{79.8}Cu_{0.1}Ga_{0.1}B_{6.1}$ alloy. As the cobalt content increases, the amount and size of phase precipitates enriched in rare-earth elements increase. Along with the main-phase grains (dark-gray phase A) in samples with x = 0 and 0.10, bright-gray phase (B) is present, which is located both at the grain boundaries and in triple junctions (Fig. 8a). Phase components with a combined structure, which consist of dark inclusions (C) surrounded by bright rims (D) (Figs. 8b–8d), appear in samples with $x \geq 0.10$. A quantitative analysis of the content of the main 2 : 14 : 1 and grain-boundary phases was performed using micrographs and linear intercept method. Table 3 (the rightmost row) shows the results of the analysis. The metallographic data show that the volume fraction of the main magnetic phase is 3–12% lower and the fraction of grain-boundary phase is two to three times higher than the volume fractions determined by X-ray diffraction analysis. Table 4 shows the results of electron microprobe analysis of the phase composition. The analysis of the reported results allows us to conclude the following characteristics of phase components.

(1) The chemical composition of the matrix in all studied magnets is close to the composition of the main magnetic 2 : 14 : 1 phase. The Co content in the

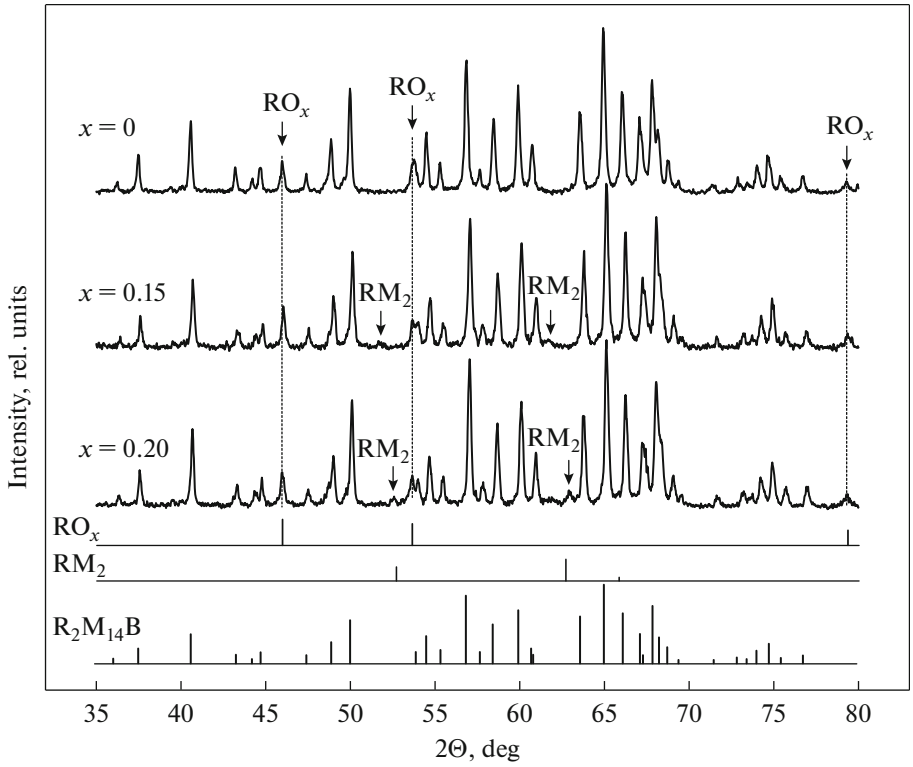

Fig. 7. X-ray diffraction patters for $(Nd_{0.75}Dy_{0.25})_{13.9}(Fe_{1-x}Co_x)_{79.8}Cu_{0.1}Ga_{0.1}B_{6.1}$ magnets.

Table 3. X-ray diffraction data for $(Nd_{0.75}Dy_{0.25})_{13.9}(Fe_{1-x}Co_x)_{79.8}Cu_{0.1}Ga_{0.1}B_{6.1}$ (R = Nd +Dy; M = Fe + Co) magnets

Co content, x	Phase	Lattice parameters, Å	Volume fraction of phase (Powder Cell Program), vol %	Volume fraction of phase (metallography), %
0	$R_2M_{14}B$	$a = 8.811$ $c = 12.123$	99	96.40
	RO_x	$a = 5.072$	1	3.60
0.15	$R_2M_{14}B$	$a = 8.777$ $c = 12.125$	96	88.90
	RO_x	$a = 5.073$	2.15	11.10
	RM_2	$a = 7.385$	1.85	
0.20	$R_2M_{14}B$	$a = 8.770$ $c = 12.116$	95.1	87.70
	RO_x	$a = 5.071$	2.51	12.30
	RM_2	$a = 7.302$	2.39	

matrix increases with increasing x, and the Co content becomes higher than that in the grains of starting alloy.

The total content of rare-earth elements in the bright-gray phase (B), the composition of which corresponds to R–M–O, decreases with increasing Co content. In this case, the stoichiometric ratio $R : M$ decreases to 1 : 2.3 at $x = 0.15$; the decrease is similar to that found for the lamellar phase in the starting alloy flakes (Table 1).

Thus, in accordance with the X-ray diffraction data, the RM_2 phase with the Laves-phase structure is stabilized in the magnets. However, the Co content in phase B is lower than that in the lamellae in the starting alloys and in the main 2 : 14 : 1 phase of the magnets. The cobalt redistribution from the grain-boundary phase into the 2 : 14 : 1 grains is likely to occur during recrystallization in the course of sintering because a part of rare-earth elements oxidizes with the formation of refractory R_2O_3 oxides. As a result, a part of cobalt, which was mainly dissolved in the lamellar phase, transfers to the main-phase grains. This agrees with the fact that the T_C temperature of magnets is slightly higher than that of starting alloys.

(2) The composition of phase B in the magnet with $x = 0.20$ (Fig. 8d) varies abruptly, which is indicated by the decrease in the stoichiometric ratio $R : M$ from 1 : 2.3 to 1 : 3.8. Electron microprobe analysis data allow us to assume that the structure of the B phase changes from the structure of the RM_2 Laves phase to the RM_4B structure ($CeCo_4B$-type structure). The formation of this phase was observed for $R_2(Fe_{1-x}Co_x)_{14}B$-based alloys with a high Co content ($x > 0.25$) [8, 16]. It is likely that, due to the abrupt decrease in the content of the main phase, which takes place as the Co content in the sintered magnet increases, the part released boron is used for the formation of the boride RM_4B phase. However, in the present study, no boride RM_4B phase was found by X-ray diffraction analysis. The widening of homogeneity range of the $RM_{2+\delta}$ Laves-phase, which takes place as the Laves phase is enriched in Co and Fe [14], is more probable.

(3) Core (C) and rim (D) of the combined phase is characterized by the higher R and oxygen contents. The structure of core C is likely to correspond to the refractory R_2O_3 phase; rim D is the former phase B with an ultimately high content of dissolved oxygen. The cobalt solubility in these phases is lower than that in phases A and B.

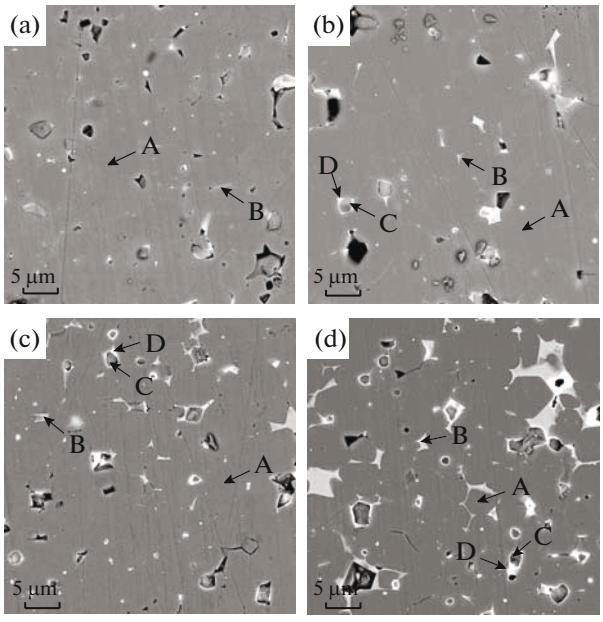

Fig. 8. Microstructure of magnets prepared from the $(Nd_{0.75}Dy_{0.25})_{13.9}(Fe_{1-x}Co_x)_{79.8}Cu_{0.1}Ga_{0.1}B_{6.1}$ alloys with different x: (a) 0, (b) 0.10, (c) 0.15, (d) 0.20.

Table 4. Electron microprobe analysis data for magnets prepared from the $(Nd_{0.75}Dy_{0.25})_{13.9}(Fe_{1-x}Co_x)_{79.8}Cu_{0.1}Ga_{0.1}B_{6.1}$ alloy (structural elements are (A) grain, (B) bright-gray phase, and combined structure consisting of (C) dark inclusions and (D) bright rims)

Co content		Phase	Chemical composition, wt %	Formula
x	wt %			
0	0	A (grain)	21.4Nd 6.2Dy 69.4Fe 1.1Co 1.2(Cu, Al, Ga) 0.7O	$RM_{7.4}O_{0.2}$
		B (bright-gray phase)	51.0Nd 11.5Dy 33.9Fe 1.1Co 1.5(Cu, Al, Ga) 1.0O	$RM_{1.6}O_{0.2}$
0.1	7.1	A (grain)	21.5Nd 4.3Dy 65.4Fe 7.8Co 0.3(Cu, Al, Ga) 0.7O	$RM_{8.0}O_{0.3}$
		B (bright-gray phase)	51.4Nd 7.2Dy 32.2Fe 5.6Co 1.6(Cu, Al, Ga) 1.0O	$RM_{1.7}O_{0.1}$
		C (dark inclusion)	55.6Nd 11.9Dy 23.2Fe 4.2Co 1.1(Cu, Al, Ga) 4.0O	$RM_{1.1}O_{0.5}$
		D (bright rim)	50.4Nd 12.9Dy 26.2Fe 4.1Co 0.6(Cu, Al, Ga) 5.8O	$RM_{1.3}O_{0.8}$
0.15	10.7	A (grain)	24.2Nd 10.1Dy 53.4Fe 10.1Co 1.4(Cu, Al, Ga) 0.8O	$RM_{5.3}O_{0.2}$
		B (bright-gray phase)	42.8Nd 10.2Dy37.9Fe 7.0Co 0.6(Cu, Al, Ga) 1.5O	$RM_{2.3}O_{0.2}$
		C (dark inclusion)	52.2Nd 12.5Dy 26.2Fe 5.0Co 0.9(Cu, Al, Ga) 3.2O	$RM_{1.3}O_{0.4}$
		D (bright rim)	54.6Nd 13.4Dy 20.8Fe 5.3Co 1.0(Cu, Al, Ga) 4.9O	$RM_{1.0}O_{0.7}$
0.20	14.2	A (grain)	21.1Nd 4.0Dy 58.8Fe 14.8Co 0.6(Cu, Al, Ga) 0.7O	$RM_{8.3}O_{0.2}$
		B (bright-gray phase)	32.6Nd 7.2Dy 40.6Fe 17.2Co 1.7(Cu, Al, Ga) 0.7O	$RM_{3.8}O_{0.1}$
		C (dark inclusion)	50.6Nd 11.0Dy 24.3Fe 7.7Co 1.4(Cu, Al, Ga) 5.0O	$RM_{1.4}O_{0.7}$
		D (bright rim)	41.1Nd 9.8Dy 31.8Fe 11.7 Co 1.5(Cu, Al, Ga) 4.1O	$RM_{2.3}O_{0.7}$

It is known from the literature data that (Nd, Dy)(Fe, Co)$_2$ Laves phases are soft magnetic ferromagnets, the Curie temperature of which is above room temperature [16, 17]. To check the presence of Laves phases, temperature dependences $\chi(T)$ were measured for samples of textured magnets in a magnetic field applied perpendicular to the texture. This approach allows us to find a small contribution from ferromagnetic phases with low both volume fraction and saturation magnetization. Figure 9 shows results of these measurements. Additional anomalies observed at 268 and 388°C were found for samples with $x = 0.15$ and 0.20, respectively.

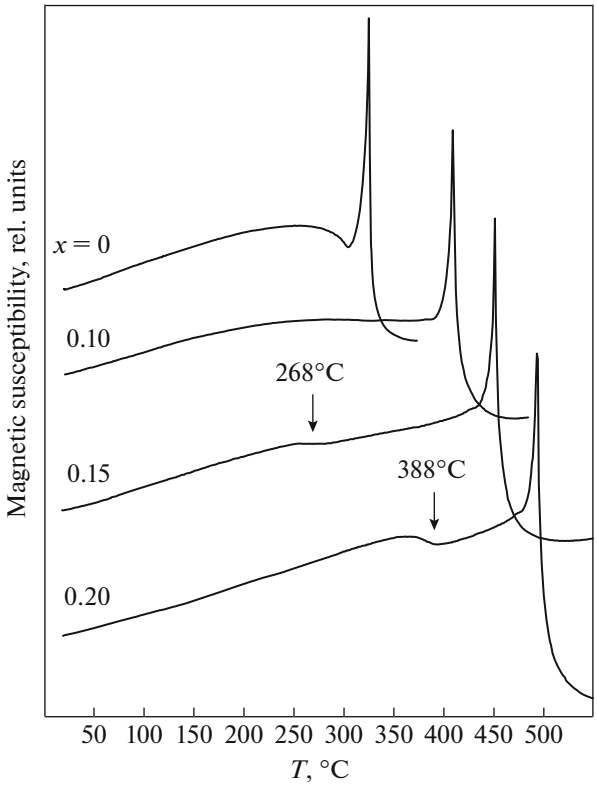

Fig. 9. Temperature dependences of magnetic susceptibility measured for sintered $(Nd_{0.75}Dy_{0.25})_{13.9}(Fe_{1-x}Co_x)_{79.8}Cu_{0.1}Ga_{0.1}B_{6.1}$ magnets across their texture.

They can be related to the formation of phases within the grain-boundary spaces, the composition of which is close to RM_2; these phases deteriorate the magnetic isolation of grains. Along with the decrease in the anisotropy field of the 2 : 14 : 1 phase, the appearance of ferromagnetic Laves phases is the cause of the substantial decrease of H_c in accordance with Eq. (3).

Effect of Alloying with Gallium on the Magnetic Properties and Microstructure

The alloying of $R_2(Fe, Co)_{14}B$-based compositions with a small amount of Ga is the well-known method to increase the coercive force of sintered magnets [16, 18–20]. Using this approach, we prepared $(Nd_{0.73}Dy_{0.27})_{14.5}Fe_{67.1}Co_{11.9}Cu_{0.1}Ga_{0.3}B_{6.1}$ ($x = 0.15$) magnets with a Ga content of 0.3%; the R content was additionally increased from 31 to 32.4 wt %. Figure 10a shows the magnetization reversal curves for this magnet, which were measured in a temperature range of 22–180°C. The temperature dependences of the B_r, H_{cJ}, and $(BH)_{max}$ parameters for magnets with $y = 0.1$

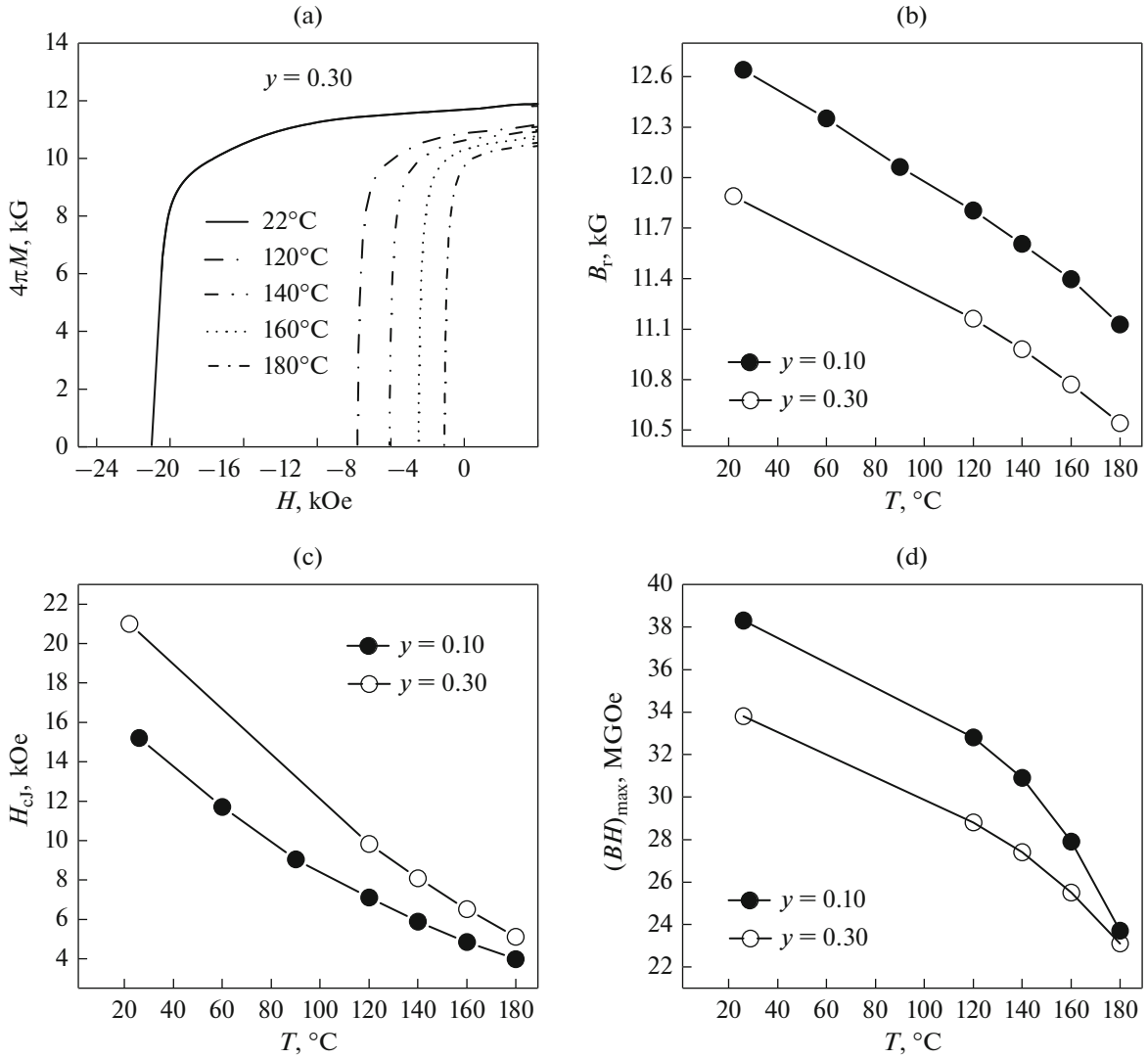

Fig. 10. (a) Magnetization reversal curves for the $(Nd_{0.73}Dy_{0.27})_{14.5}(Fe_{0.85}Co_{0.15})_{79.0}Cu_{0.1}Ga_{0.3}B_{6.1}$ ($y = 0.30$) magnet and comparison of the temperature dependences of (b) B_r, (c) H_{cJ}, and (d) $(BH)_{max}$ for sintered magnets prepared from alloys with $y =$ 0.1 and 0.3.

and 0.3 are compared in Figs. 10b–10d. It can be seen that the $B_r(T)$ and $(BH)_{max}$ dependences for magnets with 0.3% Ga lie below and the $H_{cJ}(T)$ curve lies above the analogous dependences for the magnet with 0.1% Ga. The values of temperature coefficients α and β (Table 5) for a magnet with 0.3% Ga for all temperature ranges are lower than the values for the magnet with 0.1% Ga.

Table 5. Comparison of temperature coefficients α and β for magnets prepared from the $(Nd_{0.75}Dy_{0.25})_{13.9}(Fe_{0.85}Co_{0.15})_{79.8}Cu_{0.1}Ga_{0.1}B_{6.1}$ ($y = 0.1$) and $(Nd_{0.73}Dy_{0.27})_{14.5}(Fe_{0.85}Co_{0.15})_{79.0}Cu_{0.1}Ga_{0.3}B_{6.1}$ ($y = 0.3$) alloys

T, °C	$y = 0.10$		$y = 0.30$	
	α, %/°C	β, %/°C	α, %/°C	β, %/°C
23–120	–0.071	–0.580	–0.061	–0.532
23–140	–0.072	–0.549	–0.064	–0.513
23–160	–0.074	–0.519	–0.067	–0.493
23–180	–0.078	–0.489	–0.071	–0.473

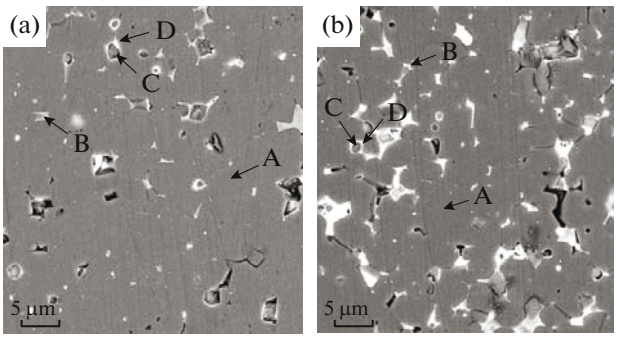

Fig. 11. Microstructure of magnets prepared from (a) $(Nd_{0.75}Dy_{0.25})_{13.9}(Fe_{0.85}Co_{0.15})_{79.8}Cu_{0.1}Ga_{0.1}B_{6.1}$ and (b) $(Nd_{0.73}Dy_{0.27})_{14.5}(Fe_{0.85}Co_{0.15})_{79.0}Cu_{0.1}Ga_{0.3}B_{6.1}$ alloys.

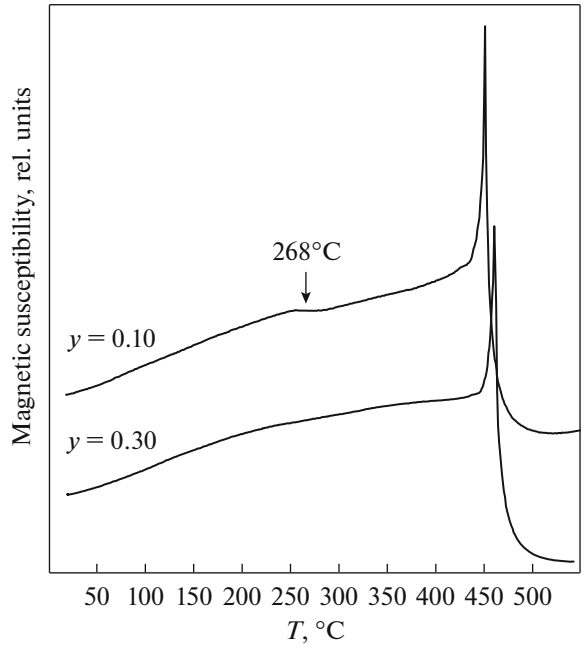

Fig. 12. Temperature dependences of magnetic susceptibility measured across the magnetic texture for the sintered $(Nd_{0.75}Dy_{0.25})_{13.9}(Fe_{0.85}Co_{0.15})_{79.8}Cu_{0.1}Ga_{0.1}B_{6.1}$ ($y = 0.1$) and $(Nd_{0.73}Dy_{0.27})_{14.5}(Fe_{0.85}Co_{0.15})_{79.0}Cu_{0.1}Ga_{0.3}B_{6.1}$ ($y = 0.3$) magnets.

A comparison of the microstructure of sintered magnets with $y = 0.1$ and 0.3 (Fig. 11) shows that the increase in the Ga and R contents leads to a marked increase in the volume fraction of the grain-boundary phases. However, in this case, the cobalt content in phase B was found to be 5 wt % lower. As a result, the grain-boundary phase of the magnet with a high Ga content consists of the paramagnetic (Nd, Dy)(Fe, Co, Ga)$_2$ phase, rather than the (Nd, Dy)(Fe, Co)$_2$ ferromagnets. This fact is indicated by the absence of bend in the dependence of magnetic susceptibility for the magnet with $y = 0.3$, which was measured across the direction of easy magnetization; however, the bend is observed for a magnet with $y = 0.1$ (Fig. 12).

Thus, the localization of Ga mainly within the grain-boundary phase and the partial substitution of Ga for Fe and Co lead to the improvement of magnetic isolation of 2 : 14 : 1-phase grains [13, 16, 21]. The other factor, which favor the positive effect of Ga on the magnetic isolation of grains, consists in the improved wetting of the grain surface with liquid during sintering [21]. All of this leads to the increase in the coercive force of the sintered $(Nd_{0.73}Dy_{0.27})_{14.5}(Fe_{0.85}Co_{0.15})_{79.0}Cu_{0.1}Ga_{0.3}B_{6.1}$ magnet in a temperature range of 23–180°C.

CONCLUSIONS

(1) The substitution of Co for Fe in the $(Nd_{0.75}Dy_{0.25})_{13.9}(Fe_{1-x}Co_x)_{79.8}Cu_{0.1}Ga_{0.1}B_{6.1}$ alloys with $x = 0$ to $x = 0.20$ allowed us to increase the Curie temperature of sintered magnets from 327 to 492°C. This favors the decrease in the modulus of the temperature coefficient of induction from 0.099 to 0.060%/°C in a temperature range of 23–140°C.

(2) As Co substitutes for Fe, the coercivity of the $(Nd_{0.75}Dy_{0.25})_{13.9}(Fe_{1-x}Co_x)_{79.8}Cu_{0.1}Ga_{0.1}B_{6.1}$ magnets at room temperature decreases from 24.6 ($x = 0$) to 14.3 kOe ($x = 0.20$). At 140°C, the H_{cJ} coercivity is only 5.58 kOe for the magnet with $x = 0.15$.

(3) The causes for the decrease in the coercivity of sintered magnets with increasing cobalt content are both the decrease in the anisotropy field of 2 : 14 : 1 magnetic-phase grains and degradation of their magnetic isolation, which is related to the formation of ferromagnetic (Nd, Dy)(Fe, Co)$_2$ Laves-phase inclusions at grain boundaries.

(4) To increase the coercive force of magnets, they were additionally alloyed with gallium; as a result, Laves-phase precipitates become ferromagnetic. Using advantages of strip casting and low-oxygen technologies, sintered magnets were prepared from the $(Nd_{0.73}Dy_{0.27})_{14.5}(Fe_{0.85}Co_{0.15})_{79.0}Cu_{0.1}Ga_{0.3}B_{6.1}$ alloy, the Curie temperature of which is high and reaches 457°C; the magnets are characterized by low value of TCI (|–0.066%/°C|). The following hysteresis characteristics of the magnet at room temperature and 140°C were reached: $B_r \geq 12.5$ kG, $H_c \geq 15$ kOe, $(BH)_{max} \geq 36$ MGOe and $B_r \geq 11.3$ kG, $H_c \geq 8$ kOe, $(BH)_{max} \geq 30$ MGOe, respectively. These characteristics of magnets correspond to world-level parameters.

ACKNOWLEDGMENTS

This study was performed within the scope of the state task of the Federal Agency for Scientific Organizations (theme “Magnet,” no. 01201463328) and was partially supported by Ural Branch, Russian Academy of Sciences (Complex program no. 15-9-2-19). X-ray diffraction studies were performed at the Collabora-

tive Access Center for Testing Nanotechnologies and Advanced Materials of the Institute of Metal Physics (Ural Branch, Russian Academy of Sciences)

REFERENCES

1. M. Sagawa, S. Fujimura, N. Togawa, H. Yamamoto, and Y. Matsuura, "New material for permanent magnets on a base of Nd and Fe," J. Appl. Phys. **55**, 2083–2087 (1984).
2. Y. Matsuura, S. Hirosawa, H. Yamamoto, S. Fujimura, and M. Sagawa, "Magnetic properties of the $Nd_2(Fe_{1-x}Co_x)_{14}B$ system," Appl. Phys. Lett. **46**, 308–310 (1985).
3. M. Sagawa, S. Hirosawa, H. Yamamoto, S. Fujimura, and Y. Matsuura, "Nd–Fe–B permanent magnet materials," Jpn. J. Appl. Phys. **26**, 785–800 (1985).
4. B. Ma and K. S. V. L.Narasimhan, "Temperature dependence of magnetic properties of Nd–Fe–B magnets," J. Magn. Magn. Mater. **54–57**, 559–562 (1986).
5. J. F. Herbst, "$R_2Fe_{14}B$ materials: Intrinsic properties and technological aspects," Rev. Modern Phys. **63**, 819–898 (1991).
6. Z. H. Hu, F. Z. Lian, M. G. Zhu, and W. Li, "Effect of Co on the thermal stability and impact toughness of sintered Nd–Fe–B magnets," J. Magn. Magn. Mater. **320**, 2364–2367 (2008).
7. W. Li, L. Jiang, D. Wang, T. Sun, and J. Zhu, "Rare-earth–transition-metal–boron permanent magnets with smaller temperature coefficients," J. Less Common Metals **126**, 95–100 (1986).
8. E. N. Kablov, A. F. Petrakov, V. P. Piskorskii, V. A. Valeev, and N. V. Nazarova, "Effect of dysprosium and cobalt on the temperature dependence of magnetization and phase composition of a material of the Nd–Dy–Fe–Co–B system," Metal Sci. Heat Treatment **49**, 159–166 (2007).
9. J. Bernardi, J. Fidler, M. Sagawa, and Y. Hirose, "Microstructural analysis of strip cast Nd–Fe–B alloys for high (*BH*)max magnets," J. Appl. Phys. **83**, 6396–6398 (1998).
10. T. Hattori, N. Fukamachi, R. Goto, N. Tezuka, and S. Sugimoto, "Microstructural evaluation of Nd–Fe–B strip cast alloys," Mater. Trans. **50**, 479–482 (2009).
11. J. Wang, Yu. Meng, H. Zhang, H. Tang, R. Lin, C. Sun, C. Wu, and F. Xie, "The characteristic of crystal growth of Nd–Fe–B cast strips during the rapid solidification process," J. Magn. Magn. Mater. **396**, 283–287 (2015).
12. A. G. Popov, T. Z. Puzanova, E. G. Gerasimov, N. B. Kudrevatykh, V. P. Vyatkin, D. Y. Vasilenko, and D. Y. Bratushev, "Preparation of high-power permanent magnets from platelike Nd–Fe–B alloys," Phys. Met. Metallogr. **109**, 238–246 (2010).
13. S. Pandian, V. Chandrasekaran, G. Markandeyulu, K. J. L. Iyer, and K. V. S. Rama Rao, "Effect of Co, Dy and Ga on the magnetic properties and the microstructure of powder metallurgically processed Nd–Fe–B magnets," J. Alloys Compds **364**, 295–303 (2004).
14. M. Sagawa, S. Hirosawa, K. Tokuhara, H. Yamamoto, S. Fujimura, Y. Tsubokawa, and R. Shimizu, "Dependence of coercivity on the anisotropy field in the $Nd_2Fe_{14}B$-type sintered magnets," J. Appl. Phys. **61**, 3559–3561 (1987).
15. J. F. Herbst and W. B. Yelon, "Preferential site occupation and magnetic structure of $Nd_2(Co_xFe_{1-x})_{14}B$ systems," *J. Appl. Phys.* **60**, 4224–4229 (1987).
16. J. Fidler, C. Groiss, and M. Tokunaga, "The influence of Ga-substitution on the coercivity of Nd–(Fe,Co)–B sintered permanent magnets," IEEE Trans. on Magn. **26**, 1948–1950 (1990).
17. K. H. J. Buschow, *Ferromagnetic Materials,* Ed. by E. P. Wohlfarth (North Holland, Amsterdam, 1980), vol. 1.
18. A. Tsutai, I. Sakai, T. Mizoguchi, and K. Inomata, "Effect of Ga addition to NdFeCoB on their magnetic properties," Appl. Phys. Lett. **51**, 1043–1045 (1987).
19. M. Tokunaga, H. Kogure, M. Endo, and H. Harada, "Improvement of thermal stability of Nd–Dy–Fe–Co–B sintered magnets by addition of Al, Nb and Ga," IEEE Trans. on Magn. **23**, 2287–2289 (1987).
20. M. Tokunaga, Y. Nozawa, K. Iwasaki, M. Endoh, S. Tanigawa, and H. Harada, "Ga added Nd–Fe–B sintered and die-upset magnets," IEEE Trans. on Magn. **25**, 3561–3566 (1989).
21. K. G. Knoch, B. Grieb, E.-Th. Henig, H. Kronmuller, and G. Petzow, "Upgraded Nd–Fe–B–*AD* (*AD* = Al, Ga) magnets: Wettability and microstructure," IEEE Trans. on Magn. **26**, 1951–1953 (1990).

Translated by N. Kolchugina